# Anomalous Rabi Oscillations in Multilevel Quantum Systems

B. Y. Chang
*School of Chemistry (BK21), Seoul National University, Seoul 08826, Republic of Korea*

I. R. Sola*
*Departamento de Química Física I, Universidad Complutense, 28040 Madrid, Spain*

Vladimir S. Malinovsky†
*U.S. Army Research Laboratory, Adelphi, Maryland 20783, USA*

(Received 27 August 2017; published 27 March 2018)

We show that the excitation probability of a state within a manifold of levels undergoes Rabi oscillations with the frequency determined by the energy difference between the states and not by the pulse area, for sufficiently strong pulses. The population and coherence remains in the two-level subsystem formed by the initial and target state even at Rabi frequencies exceeding the energy difference. The observed dynamics can be useful in nonlinear spectroscopy and quantum state preparation.

DOI: 10.1103/PhysRevLett.120.133201

Coherent excitation is a fundamental step for quantum state preparation, underlying a variety of implementations in quantum information and quantum control of atoms, molecules, and nanodevices. In general, quantum systems have complex structures; however, under certain conditions, their dynamics can be well described by just a few separated energy levels [1–3]. In this regard, the two-level structure (TLS) represents a particularly simple and well-adapted system to represent a qubit or to describe elementary control processes [4,5].

In some cases, dressing a quantum system in slowly changing fields allows us to use the adiabatic representation and reduces the complicated multilevel dimensionality to just one or a few dressed states [6–8]. This is the case of the stimulated Raman adiabatic passage (STIRAP) [9], its generalizations for $N$-level systems with more complex structures [6,7,10], and molecular wave packets [11,12]. Adiabatic control methods have also found interesting applications in quantum gate design [13] and control of entanglement [14–16]. It is instructive to note a recent discussion regarding the important role of the nonadiabatic couplings in STIRAP [17] and other control techniques, such as coherent destruction of tunneling [18].

Here, we report unexpected results found during a reexamination of the pulse area theorem [1,19,20] in TLS and multilevel systems, where the additional off-resonant levels do not participate, in principle, in the population transfer. Under a constant field of amplitude $\epsilon_0$ and frequency $\omega$, slightly detuned from the resonance, so that $\Delta = E_2 - E_1 - \hbar\omega$, the excitation probability of the TLS undergoes Rabi oscillations

$$P_2(t) = \frac{\Omega_0^2}{\Omega_{\text{eff}}^2} \sin^2(\Omega_{\text{eff}} t/2), \tag{1}$$

where $\Omega_0 = \mu\epsilon_0$ is the Rabi frequency (in atomic units), and the effective Rabi frequency $\Omega_{\text{eff}} = \sqrt{\Omega_0^2 + \Delta^2}$ takes into account the effect of the detuning. The detuning accelerates the rate of the population transfer but decreases the maximum that can reach the target state, hampering the efficiency and robustness of the preparation process. A general feature of detuning is to generate fast oscillating dynamical phases that modulate (and reduce) the coherent transfer induced by the Rabi frequency.

Logically, we may expect that increasing the system complexity will make it more difficult to control the population dynamics, since more states will be involved and more effective detunings will modulate the Rabi oscillations. Indeed, one of the main problems of building quantum machines (e.g., quantum computers) is the ability to first isolate TLS and then couple these structures in a controllable way. In this Letter, however, we show that there are very general classes of structures, more complex than the TLS, where the additional states help to enhance the robustness of the population transfer. It turns out that, in the presence of a driving field, the system dressed states are characterized by isolating a "two-level dressed substructure" (TLDS) where the dynamics occurs. Assuming constant fields for simplicity, the effective Rabi frequency driving the population dynamics within these two dressed states is of the form

$$\Omega_{\text{eff}} = \sqrt{a\delta^2 + b\Omega_0^2 - \sqrt{a^2\delta^4 + b^2\Omega_0^2 + c\delta^2\Omega_0^2}}, \tag{2}$$

where $\delta$ is a characteristic energy splitting of the system, and $a$, $b$, $c$ are some relevant parameters. Whereas the dynamics of the ordinary TLS is governed by the largest

 

system frequency (the Rabi frequency or the detuning), in the TLDS, the behavior is just the opposite; the driving force is always the slowest system frequency, given $\Omega_0$ at low field intensities, and by $\delta$, at large intensities. This self-regulated behavior makes these systems promising candidates from which to build quantum machines, owing to the greater robustness of their coherent population dynamics. Note that, in this case, the speed of quantum operations (gates) is constrained by the energy splitting of the system and not by the strength of the external drive. We will refer to the oscillations induced by the effective Rabi frequency of the form of Eq. (2) or its time-dependent generalizations as anomalous Rabi oscillations (AROs).

Although AROs occur in very general scenarios, we first focus on highly symmetrical systems where analytical solutions can be found. Let us consider a four-level tripod system composed of three nondegenerate levels in the ground state coupled to a single excited state. A possible experimental realization could be the excitation from a $J = 1$ atomic state to an excited $J = 0$ state by the fields of a suitable polarization to allow all the couplings. In particular, a field with elliptical polarization $\vec{\mathcal{E}}(t) = \mathcal{E}_0(t)(\hat{k} - i\sqrt{2}\hat{j})/\sqrt{3}$ (where $\hat{j}, \hat{k}$ are unit vectors along $y, z$, and $\mathcal{E}_0(t)$ is the pulse envelope) guarantees that all couplings are of equal magnitude. In fact, since the ARO does not depend on the sign of the Rabi frequencies, different field polarizations obtained from a superposition of two orthogonal electric fields of different amplitude can be used. A very specific arrangement is only needed to reproduce the conditions of the analytic Hamiltonian. The degeneracy of the ground sublevels can be lifted by a strong magnetic field directed along the $z$ axis that creates Zeeman splittings $\delta = g\mu_B B$, where $g$ is the Landé factor, $\mu_B$ is the Bohr magneton, and $B$ is the magnetic field. Here we are interested in the regime where the splittings are larger than the pulse bandwidth and we assume that any Zeeman sublevel of the ground state can be initially prepared. A similar behavior occurs when $J = 0$ is the initial state and $J = 1$ is the final state.

Expanding the wave function as $|\Psi(t)\rangle = \sum_{M=-1}^{1} a_M(t)|M\rangle + a_{0'}(t)|0'\rangle$, where $M$ is the magnetic quantum number in the ground state and the prime indicates the excited state, and applying the rotating wave approximation (RWA) in the field interaction representation, the Hamiltonian can be written as

$$\mathsf{H} = \sum_M \delta M|M\rangle\langle M| + \Delta|0'\rangle\langle 0'| - \Omega(t)/2 \times \left(\sum_M |M\rangle\langle 0'| + \text{H.c.}\right), \tag{3}$$

where $\Delta = E_{0'} - \hbar\omega$ is the single-photon detuning, $\omega$ is the carrier frequency, $\Omega(t) = \Omega_0 \exp\{-(t - t_c)^2/(2\tau_0^2)\}$, $\Omega_0$ is the peak Rabi frequency, $\tau_0$ determines the pulse duration,

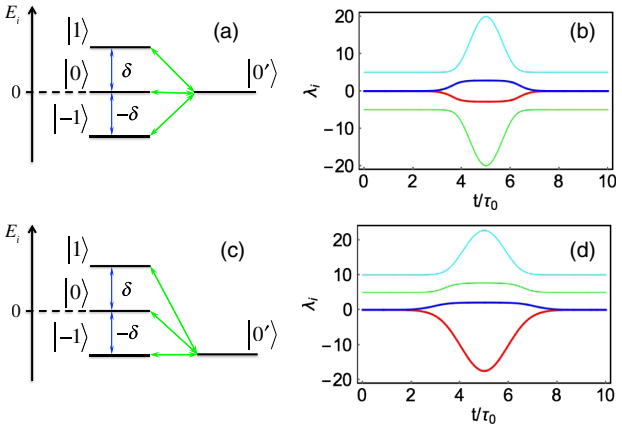


FIG. 1. Tripod system in symmetric (a) and asymmetric (c) configurations and their respective dressed states (b) and (d); $t_c = 5\tau_0$, $\delta\tau_0 = 5$, $\Omega_0\tau_0 = 18$. The thicker blue and red lines correspond to the populated dressed states.

and H.c. refers to the Hermitian conjugate components. Choosing $\Delta = \delta M$, we can resonantly excite the $|0'\rangle$ state from any initial sublevel. Starting in the $|0\rangle$ sublevel, we obtain the most symmetrical arrangement when $\Delta = 0$. Figure 1 shows a sketch of the system, including the couplings for the symmetrical arrangement (a) as well as one possible asymmetric configuration (b), where $\Delta = -\delta$. In the figure, we also present the time-dependent energies of the system dressed states for both configurations.

In the adiabatic limit, the dynamics of the system in the symmetric configuration can be described analytically. By diagonalizing the Hamiltonian, Eq. (3), we obtain the time-dependent energies of the dressed states $\lambda_{1,2}(t) = \mp\sqrt{\Lambda_-/2}$, $\lambda_{3,4}(t) = \mp\sqrt{\Lambda_+/2}$, with $\Lambda_\mp = \delta^2 + 3\chi^2 \mp D^2$, where $D^2 = \sqrt{\delta^4 + 2\chi^2(t)\delta^2 + 9\chi^4(t)}$, $\chi(t) = \Omega(t)/2$. From these expressions, we see two limiting cases: for the weak fields, when $\Omega_0 \ll \delta$, $\lambda_{1,2}(t) = \mp\chi(t)$, while for large pulse intensities, $\Omega_0 \gg \delta$, $\lambda_{1,2}(t) = \mp\delta/\sqrt{3}$. We also observe that the dressed states come in pairs: the distance between $\lambda_1(t)$ and $\lambda_2(t)$ is approximately bounded by the energy splitting due to avoided crossings with the other dressed states, and it remains small regardless of the pulse amplitude, while the distance between $\lambda_3(t)$ and $\lambda_4(t)$ increases following the Rabi frequency $\Omega(t)$.

For the initial condition $a_0(0) = 1$, the wave function at the end of the pulse depends only on the amplitudes $a_0$ and $a_{0'}$. Neglecting nonadiabatic couplings, the analytic solution of the time-dependent Schrödinger equation (TDSE) is

$$a_0(t) = \frac{2\chi^2(t)}{D\sqrt{D^2 - \delta^2 - \chi^2(t)}} \cos\left(\int_0^t \lambda_2(t')dt'\right), \tag{4}$$

$$a_{0'}(t) = \frac{2i\delta\chi(t)}{D\sqrt{D^2 - \delta^2 + 3\chi^2(t)}} \sin\left(\int_0^t \lambda_2(t')dt'\right). \tag{5}$$

At the end of the pulse ($t = T$), the target state population follows the area theorem $P = \sin^2(\mathcal{A}/2)$ with a generalized area $\mathcal{A} = 2\int_0^T dt\lambda_2(t)$. While for small pulse intensities ($\Omega_0 \ll \delta$), $\mathcal{A} \approx \int_0^T dt\Omega(t) = S_0$, it asymptotically approaches a constant value at large intensities. A coherent saturation effect makes the yield of population transfer much more robust as the field intensity increases, contrary to the standard TLS result [1]. In practice, this leads to very slow oscillations in the final state, which are controlled by the Zeeman splitting $\delta$.

Figure 2(a) compares the final yield as a function of $S_0$ in the adiabatic limit (analytic results) with the result of numerical integration of the TDSE. We have used Gaussian pulses with $\delta\tau_0 = 5$. The agreement of the results shows that the nonadiabatic couplings are negligible until $\Omega_0 \ll \delta$, when the states $|\pm 1\rangle$ also become populated at the final time. Surprisingly, in the TLDS, the adiabaticity is damaged at large pulse intensities, in contrast to the commonly accepted adiabatic criterion [6,7].

Figure 2(b) shows a density plot of the final yield of population transfer as a function of both $S_0$ and $\delta$, calculated numerically. For not very large Rabi frequencies, the final-time population oscillates between the initial and the target state as it is in the traditional TLS. The states $|\pm 1\rangle$ are only populated due to nonadiabatic couplings, leading first to some higher-frequency modulation or wiggles of the ARO and lower yields, and then to some enlargement of the oscillation period since part of the pulse energy is used to excite other Zeeman levels via Raman transitions. These effects are due to some population transfer near the crossings of $\lambda_{1,2}(t)$ with $\lambda_{3,4}(t)$, when $\Omega(t) \approx \delta$ at the beginning and end of the pulse. Hence, the nonadiabatic effects are less important the larger the energy splitting is.

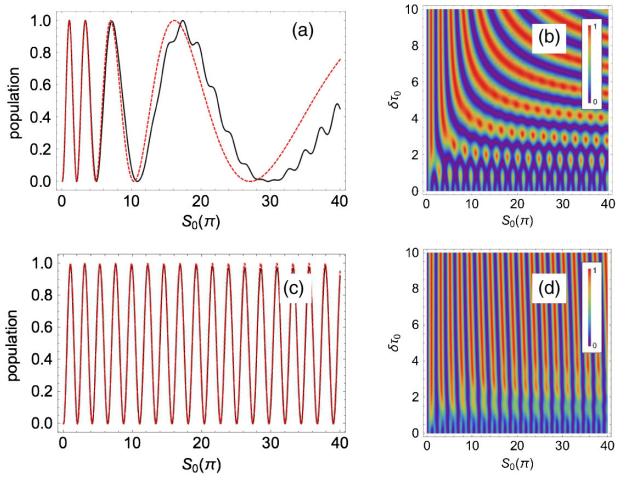


FIG. 2. Coherent population transfer to the target state in the symmetric (a) and asymmetric (c) tripod schemes, as a function of the pulse area, for $\delta\tau_0 = 5$. The red dotted line represents the analytical results (neglecting nonadiabatic couplings) and the black solid line represents the numerical solution of the TDSE. (b), (d) The target population at final time $T$ as a function of both pulse area $S_0$ and splitting $\delta$.

The presence of the ARO requires the isolation of a TLDS, which depends on the linking patterns of the system. For instance, if we choose to start in the $|\pm 1\rangle$ levels, fixing the detuning accordingly ($\Delta = \pm\delta$), as shown in Fig. 1(b), then we observe the regular Rabi oscillations that basically depend on the pulse area. This is because the populated dressed states $\lambda_1(t)$ and $\lambda_3(t)$ are the lowest pair [see Fig. 1(d)], and the generalized pulse area $\mathcal{A} = \int_0^T dt[\lambda_1(t) - \lambda_3(t)]$ is dominated by the dynamic phase accumulated by the lowest dressed state, whose Autler-Townes splitting approximately follows the field envelope. In the adiabatic limit, we can obtain analytic results for the asymmetric configuration, although the expressions are more cumbersome and are not presented here. In Fig. 2(c), we compare the analytical results with the exact numerical solution of the TDSE showing full coincidence. Figure 2(d) shows the density plot of the final yield of population transfer as a function of $S_0$ and $\delta$, calculated numerically from the TDSE.

What is essentially required to observe an ARO? As previously mentioned, we need to isolate the TLDS among the set of all levels. This implies using relatively long pulses, with a bandwidth smaller than the energy spacing, such that there is no transient absorption to other states induced by the lack of energy resolution. The initial and target states cannot both be the highest or lowest energy eigenstates of their respective manifolds. Hence, a minimum number of four coupled levels are needed, but there is no upper limit on the number of states. In the following, we report representative results for two more complex systems. We first consider population transfer in a system of two fully coupled five-level ladders, with Hamiltonian

$$\mathsf{H} = \sum_M \delta M|M\rangle\langle M| + \sum_{M'}(\delta' M' + \Delta)|M'\rangle\langle M'| - \Omega(t)/2 \times \left(\sum_{M,M'}|M\rangle\langle M'| + \text{H.c.}\right), \tag{6}$$

where $M$, $M' = \pm 2$, $\pm 1$, 0, and $\delta$, $\delta'$ are the energy splittings of the ground and excited manifolds. The left column of Fig. 3 shows the population of the target state as a function of the pulse area when we start in the $|0\rangle$ state to reach the target state $|0'\rangle$ using $\Delta = 0$ or the target state $|-2'\rangle$ using $\Delta = -2\delta'$. If the transition is not resonant, an additional detuning modulates the oscillation and affects the maximum population transfer that can be achieved, as in Eq. (1). When the pulse duration is on the order of the period associated with the energy splitting, the population flow is not fully selective, but one can still observe AROs between the overall population of the manifolds. For shorter pulses, we observe normal Rabi oscillations and lower yields, due to Raman transitions.

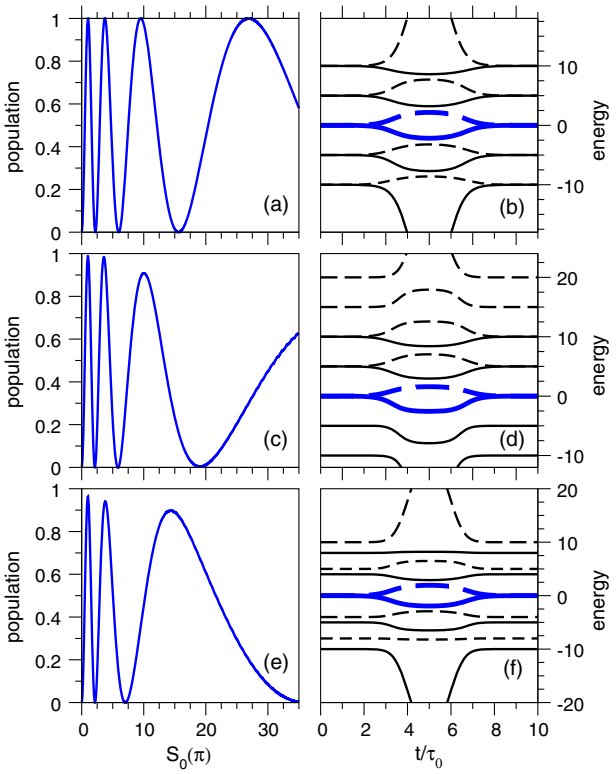


FIG. 3. Target population at final time as a function of the pulse area (left column) and the corresponding dressed states for $\Omega_0\tau_0 = 10$ (right column) in a system of two coupled five-level ladders with $\delta\tau_0 = 5$. (a), (b) We start and end in the middle of the ladder ($M = M' = 0$). (c), (d) We start in the middle and end at the lowest level of the ladder ($M' = -2$). (e), (f) The target ladder has a different energy splitting ($\delta' = 4$). The populated dressed states are always shown with thicker blue lines.

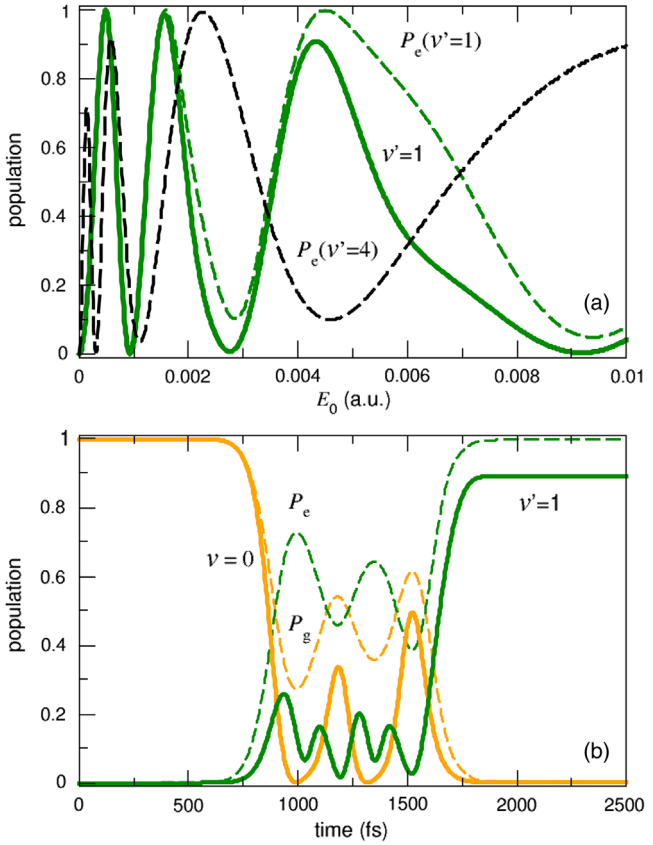


FIG. 4. (a) Electronic excited state populations $P_e$ (dashed lines) for two different target vibrational states $v' = 1$ and $v' = 4$ of the excited electronic state of $Na_2$, as a function of the pulse amplitude; population of vibrational state $v' = 1$ of the excited electronic state (solid line). (b) Population dynamics for the electronic transition $v = 0$ to $v' = 1$ using $E_0 = 0.0045$ a.u. The solid lines are the populations in the initial and target vibrational states, while the dashed lines are the electronic populations $P_g$ and $P_e$.

The right column of Fig. 3 shows the corresponding dressed states when $\Omega_0\tau_0 = 10$. The symmetric arrangement minimizes the nonadiabatic couplings isolating the TLDS and a perfect ARO is observed [Figs. 3(a) and 3(b). Asymmetries cause larger couplings that lead to some distortions in the ARO and losses in the yield of population inversion [Figs. 3(c) and 3(d)]. A similar effect is observed if the Rabi frequencies among the different levels are not equal. Figures 3(e) and 3(f) show the change in the ARO when the energy splittings in the manifolds are different. In general, an ARO will occur when the populated dressed states are constrained by avoided crossings with the near-lying dressed states, which will happen as long as there are no strong selection rules that forbid most couplings, generating block-diagonal Hamiltonians. This is the case, for instance, in higher angular momentum states ($M \geq 2$), where the selection rule $\Delta M = \pm 1$ will forbid the ARO by breaking the necessary linking couplings. In addition, if the dipole couplings decrease quickly in the manifold as $\Delta M$ increases, the nonadiabatic couplings cannot be neglected and the pattern of the ARO becomes more complex.

To further illustrate the universality of the AROs, we next consider electronic excitation from the ground state $^1\Sigma_g$ to the first excited state $^1\Sigma_u$ in the $Na_2$ dimer. Here, the Franck-Condon couplings for the different state-to-state transitions are quite diverse, as are the energy splittings due to anharmonicities and differences in the ground and excited potential energy curves of the molecule. In Figure 4(a), we show the final electronic population (which could be tracked by the overall fluorescence) as a function of the pulse peak amplitude $E_0$ and the relevant vibrational population. We use Gaussian pulses of 500 fs duration (FWHM) with carrier frequencies resonant to the chosen target vibrational state ($v' = 1$ and $v' = 4$ in the chosen examples). In the simulations, we use realistic *ab initio* potentials and transition dipoles [12], but we neglect transitions to higher excited electronic states and ionization, which may affect the dynamics at the larger intensities. The field must be quite intense, as the chosen transitions are below the Franck-Condon region, where the coupling is highest ($\sim v' = 8$). In Fig. 4(b), we show an example of the population histories with $E_0 = 0.0045$ a.u., at the

maximum of the third Rabi oscillation. The breakdown of the adiabatic conditions for large $E_0$ leads to considerable transient excitation of other vibrational states of the ground and excited potential. Although less state selective, full electronic AROs are clearly observed in spite of the complexity of the system.

In summary, we have shown a new generic effect of coherent excitation of quantum systems. Under strong excitation with long pulses (areas typically larger than $2\pi\delta$), two-level dressed states are isolated by avoided crossing with the remaining dressed states of the system. When the initial or target states are embedded in a manifold of levels, the Rabi oscillation frequency of the populations depend on the characteristic energy splitting and not on the pulse area. At the final time, the population and coherence remains in the two-level subsystem formed by the initial and target state, showing that the robustness of state preparation by Rabi oscillations exceeds what was previously expected. In addition, the sensitivity of the ARO to the energy splittings could in principle be used to obtain the parameters of the Hamiltonian, even when the additional levels in the manifold are never (or very weakly) populated at the final time. Thus, coherent population dynamics via the ARO could be used as a new spectroscopic method.

This work was supported by the Korean government through the Basic Science Research program (2017R1A2B1010215) and by the Spanish government through the MINECO Project No. CTQ2015-65033-P.

*isola@quim.ucm.es
†vladimir.s.malinovsky.civ@mail.mil

[1] L. Allen and J. H. Eberly, *Optical Resonance and Two-Level Atoms* (Dover, New York, 1975).
[2] M. O. Scully and M. S. Zubairy, *Quantum Optics* (Cambridge University Press, Cambridge, 1997).
[3] P. R. Berman and V. S. Malinovsky, *Principles of Laser Spectroscopy and Quantum Optics* (Princeton University Press, Princeton, 2011).
[4] M. A. Nielsen and I. L. Chuang, *Quantum Computation and Quantum Information* (Cambridge University Press, Cambridge, 2006).
[5] M. Schapiro and P. Brumer, *Quantum Control of Atoms and Molecules* (Cambridge University Press, Cambridge, 1997).
[6] K. Bergmann, H. Theuer, and B. W. Shore, Rev. Mod. Phys. **70**, 1003 (1998).
[7] N. V. Vitanov, A. A. Rangelov, B. W. Shore, and K. Bergmann, Rev. Mod. Phys. **89**, 015006 (2017).
[8] B. W. Shore, *Manipulating Quantum Structures Using Laser Pulses* (Cambridge University Press, Cambridge, 2011).
[9] U. Gaubatz, P. Rudecki, S. Schiemann, and K. Bergmann, J. Chem. Phys. **92**, 5363 (1990).
[10] V. S. Malinovsky and D. J. Tannor, Phys. Rev. A **56**, 4929 (1997).
[11] B. M. Garraway and K.-A. Suominen, Phys. Rev. Lett. **80**, 932 (1998).
[12] I. R. Sola, B. Y. Chang, J. Santamaria, V. S. Malinovsky, and J. L. Krause, Phys. Rev. Lett. **85**, 4241 (2000).
[13] V. S. Malinovsky, I. R. Sola, and J. Vala, Phys. Rev. A **89**, 032301 (2014).
[14] V. S. Malinovsky and I. R Sola, Phys. Rev. Lett. **93**, 190502 (2004).
[15] V. S. Malinovsky and I. R. Sola, Phys. Rev. A **70**, 042304 (2004).
[16] V. S. Malinovsky and I. R. Sola, Phys. Rev. A **70**, 042305 (2004).
[17] Y. Sun and H. Metcalf, Phys. Rev. A **90**, 033408 (2014).
[18] F. Grossmann, T. Dittrich, P. Jung, and P. Hänggi, Phys. Rev. Lett. **67**, 516 (1991).
[19] G. Shchedrin, C. O'Brien, Y. Rostovtsev, and M. O. Scully, Phys. Rev. A **92**, 063815 (2015).
[20] M. Holthaus and B. Just, Phys. Rev. A **49**, 1950 (1994).